

Transient electrically detected magnetic resonance spectroscopy applied to organic solar cells

Felix Kraffert, Robert Steyrlleuthner, Christoph Meier, Robert Bittl, and Jan Behrends

Citation: [Applied Physics Letters](#) **107**, 043302 (2015); doi: 10.1063/1.4927446

View online: <http://dx.doi.org/10.1063/1.4927446>

View Table of Contents: <http://scitation.aip.org/content/aip/journal/apl/107/4?ver=pdfcov>

Published by the [AIP Publishing](#)

Articles you may be interested in

[Magnetic field effect spectroscopy of C60-based films and devices](#)

J. Appl. Phys. **113**, 143102 (2013); 10.1063/1.4800546

[Carrier recombination losses in inverted polymer: Fullerene solar cells with ZnO hole-blocking layer from transient photovoltage and impedance spectroscopy techniques](#)

J. Appl. Phys. **109**, 074514 (2011); 10.1063/1.3561437

[Electrical characterization of single-walled carbon nanotubes in organic solar cells by Kelvin probe force microscopy](#)

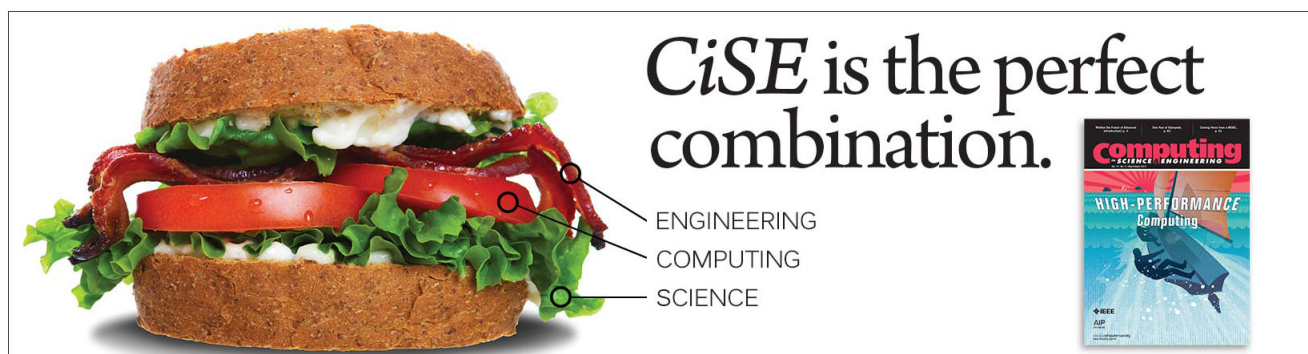
Appl. Phys. Lett. **96**, 083302 (2010); 10.1063/1.3332489

[Antenna effects and improved efficiency in multiple heterojunction photovoltaic cells based on pentacene, zinc phthalocyanine, and C 60](#)

J. Appl. Phys. **106**, 064511 (2009); 10.1063/1.3187904

[Efficient organic solar cells by penetration of conjugated polymers into perylene pigments](#)

J. Appl. Phys. **96**, 6878 (2004); 10.1063/1.1804245

The advertisement is enclosed in a thin black border. On the left is a large, detailed image of a sandwich with lettuce, tomato, and meat. On the right, the text 'CiSE is the perfect combination.' is written in a large, black, serif font. Below this text are three lines: 'ENGINEERING', 'COMPUTING', and 'SCIENCE', each preceded by a small black circle and a thin line pointing to a corresponding part of the sandwich. To the right of the text is a small image of a journal cover titled 'Computing SCIENCE ENGINEERING' with the subtitle 'HIGH-PERFORMANCE Computing' and an image of a blue submarine.

Transient electrically detected magnetic resonance spectroscopy applied to organic solar cells

Felix Kraffert, Robert Steyrlleuthner, Christoph Meier, Robert Bittl, and Jan Behrends^{a)}
 Berlin Joint EPR Lab, Fachbereich Physik, Freie Universität Berlin, D-14195 Berlin, Germany

(Received 24 April 2015; accepted 15 July 2015; published online 27 July 2015)

The influence of light-induced paramagnetic states on the photocurrent generated by polymer:fullerene solar cells is studied using spin-sensitive techniques in combination with laser-flash excitation. For this purpose, we developed a setup that allows for simultaneous detection of transient electron paramagnetic resonance as well as transient electrically detected magnetic resonance (trEDMR) signals from fully processed and encapsulated solar cells. Combining both techniques provides a direct link between photoinduced triplet excitons, charge transfer states, and free charge carriers as well as their influence on the photocurrent generated by organic photovoltaic devices. Our results obtained from solar cells based on poly(3-hexylthiophene) as electron donor and a fullerene-based electron acceptor show that the resonant signals observed in low-temperature ($T=80$ K) trEDMR spectra can be attributed to positive polarons in the polymer as well as negative polarons in the fullerene phase, indicating that both centers are involved in spin-dependent processes that directly influence the photocurrent. © 2015 AIP Publishing LLC. [<http://dx.doi.org/10.1063/1.4927446>]

Photocurrent generation in solar cells based on organic semiconductors (OS) often involves localized states which, if occupied by single electrons or holes, are paramagnetic and can be detected by electron paramagnetic resonance (EPR) spectroscopy.^{1,2} Since OS typically comprise rather light atoms, spin-orbit coupling is small, and spin-relaxation times are long, approaching microseconds at room temperature in some materials.^{3,4} The spin degree of freedom can thus decisively influence charge transfer (CT) and charge separation processes in organic solar cells (OSC).⁵ EPR techniques are capable of detecting separated polarons, weakly coupled CT states as well as triplet excitons.^{2,6–8} Further, EPR spectroscopy allows studying the dynamics of the conversion between these different types of excited states.⁹ Transient EPR (trEPR) spectroscopy turned out to be particularly useful for this purpose. This technique measures time-resolved EPR signals after a laser-flash excitation and, for instance, was successfully applied to investigate triplet exciton generation as possible loss channel in blends consisting of low-bandgap polymers and fullerene-based electron acceptors.¹⁰

While EPR-based techniques can provide valuable insight into excitation transfer pathways in OS used as absorber layers in solar cells, drawing conclusions on processes relevant under solar-cell operating conditions is oftentimes not trivial, mainly because of the following difficulties:

- (1) It is often not clear whether the paramagnetic species probed by EPR are relevant for solar cell operation or represent just a minor subspecies without any influence on the photocurrent.
- (2) EPR measurements are mostly performed on samples with geometries differing from those of solar cells. For

instance, studying rather thick OS films can increase the signal-to-noise ratio in EPR experiments. However, the properties of thick films ($>1 \mu\text{m}$) with respect to, e.g., the nano-morphology may substantially differ from those of thin films used in fully processed solar cells.

- (3) The biasing conditions, e.g., whether charge carriers are injected or extracted, can affect the dynamics of the paramagnetic species and decisively influence the free charge carrier yield. EPR measurements performed on solar cell absorber materials without electrodes, which are essentially carried out under open circuit conditions, may thus detect other processes and paramagnetic species than those dominating in an operating solar cell.

In order to lift these restrictions, we developed the technique of transient electrically detected magnetic resonance (trEDMR) that combines the time resolution of trEPR¹¹ and the unprecedented detection sensitivity of EDMR spectroscopy.¹² This technique usefully complements continuous wave and pulsed EDMR (cwEDMR and pEDMR) that are successfully applied to study spin-dependent charge transport and recombination processes in organic and inorganic semiconductors.^{13–15} Our setup allows for simultaneous detection of trEPR and trEDMR (as illustrated schematically in Fig. 1(a)) from fully processed and encapsulated organic solar cells. Combining both spin-sensitive techniques provides a direct link between triplet excitons, CT states, and free charge carriers as well as their influence on the photocurrent in polymer:fullerene blends. The usefulness of this approach is demonstrated by measurements performed on bulk heterojunction solar cells made from the archetypical materials poly(3-hexylthiophene) (P3HT) and [6,6]-phenyl C61-butyric acid methyl ester (PCBM).

The absorber layers of the miniaturized solar cells for EPR and EDMR were fabricated by spin-coating (1500 rpm for 30 s) inside an inert atmosphere glovebox from chlorobenzene solution (20 g/l, weight ratio 1:1) onto glass

^{a)}Author to whom correspondence should be addressed. Electronic mail: j.behrends@fu-berlin.de.

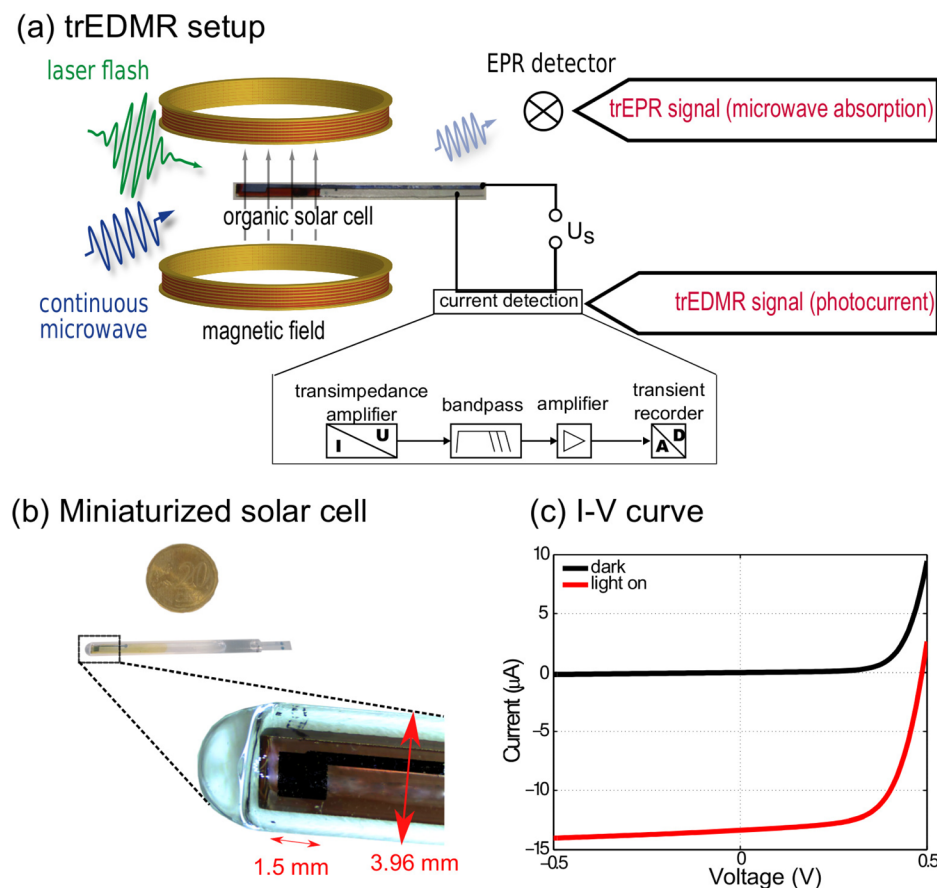


FIG. 1. (a) Schematic illustration of a combined transient EDMR and transient EPR experiment. (b) Photograph of a miniaturized organic solar cell compatible with transient EDMR measurements. (c) I - V characteristics of the solar cell measured inside an EPR resonator at room temperature.

substrates covered with structured indium tin oxide and an additional 50 nm poly(3,4-ethylenedioxythiophene) polystyrene sulfonate layer (spin-coated at 1500 rpm for 30 s). The films have been subsequently annealed at $T = 120^\circ\text{C}$ for 10 min. The regio-regular P3HT was purchased from Rieke Metals and the PCBM from Solenne. The solvent as well as the weight ratio was chosen such that the properties of the resulting films are suitable for reliably working solar cell devices.^{16–18} The back-electrodes were processed by thermal evaporation at a base pressure of $\leq 2 \times 10^{-6}$ mbar and consist of a 10 nm thick Ca layer followed by 150 nm Al. The working organic solar cells were placed into short quartz tubes with an outer diameter of 4 mm and were sealed under nitrogen atmosphere (glovebox-based preparation) with a two component epoxy resin (Emerson and Cuming STYCAST 1266). A photograph of the encapsulated solar cell is shown in Fig. 1(b). The oxygen-free preparation and storage of the solar cells are necessary since OSC tend to degrade rapidly when being exposed to oxygen and light.^{19,20}

The current–voltage characteristics shown in Fig. 1(c) were recorded with a sourcemeter (Keithley 2611A) at room temperature. For this purpose, the solar cell was placed inside an EPR resonator and illuminated by a stabilized white-light source (Polytec DCR IV).

Transient EPR and EDMR spectra were recorded using a laboratory-built combined X-/Q-band EPR spectrometer and a dielectric ring resonator (Bruker ER 4118X-MD5). The magnetic field axis was calibrated by a Gaussmeter (Bruker ER 035M), and the (constant) offset between the positions of the Gaussmeter and the sample was determined by a reference sample (nitrogen encapsulated in C_{60}).

Optical excitation at $\lambda = 532$ nm (close to the absorption maximum of P3HT) was provided by a diode-pumped Nd:YAG laser (Atum Laser Titan AC compact 15 MM) equipped with a second harmonic generator. The pulse length was 5 ns, and the fluence used was approximately 1.5 mJ/cm^2 .

The transient EPR and EDMR experiments were performed at $T = 80$ K, because the trEPR signals of P3HT:PCBM blends are well studied at this temperature,⁹ whereas no room-temperature trEPR data are available for this material. Cooling was provided by a laboratory-built helium-gas flow cryostat. The bias voltage was set to $U = 0.77$ V, leading to a negative current response after the laser flash as shown in Fig. 3. The bias voltage was supplied by a combined power supply and current amplifier (Elektronik Manufaktur Mahlsdorf). The response time of the current detection is limited by the current amplifier as well as the resistance and the capacitance of the solar cell and the connection lines under the respective operating conditions. The amplified current transients were recorded by a digital oscilloscope (LeCroy WaveRunner 104MXi). The signal acquisition was triggered by the laser flash using a fast photodiode. Several EDMR transients were accumulated for each position in the scan range of the static magnetic field. The time between subsequent laser pulses was 10 ms. The non-resonant background signal induced by the laser flash recorded far from the resonant signal was subtracted from each EPR and EDMR transient.

Transient EPR signals (microwave-detected instead of current-detected) were recorded under identical conditions as described previously.⁹

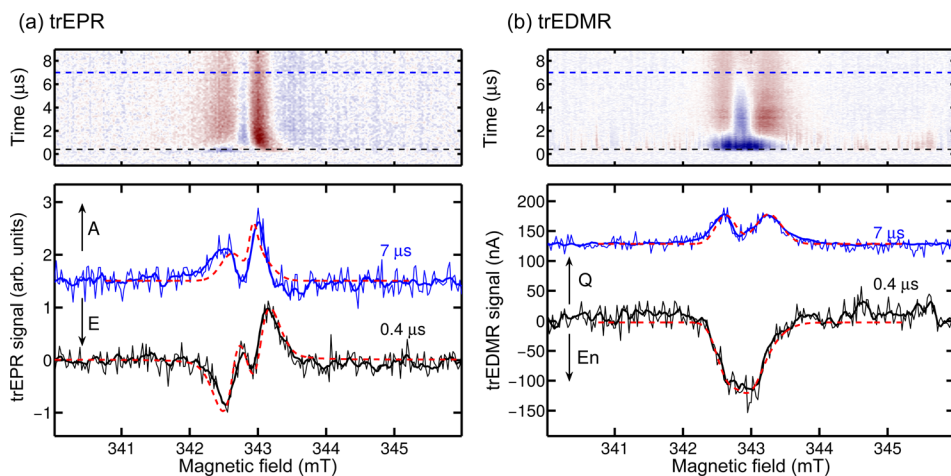


Fig. 2 shows the results of (a) trEPR and (b) trEDMR measurements performed on the same fully processed solar cell at a microwave frequency of ~ 9.6 GHz. The upper panel in Fig. 2(a) shows the color-encoded (red: absorption and blue: emission) time evolution of the trEPR signal after the laser flash at $t=0$ vs. the magnetic field. The lower panel displays two slices along the field axis at $0.4 \mu\text{s}$ and $7 \mu\text{s}$ after the laser flash. The EAEA-signature (A: absorptive, E: emissive) observed at $t=0.4 \mu\text{s}$ can be attributed to spin-correlated polaron pairs, i.e., CT states at the donor/acceptor interface.⁹ The purely absorptive signal detected for longer delays resembles the spectrum of two uncoupled polarons. Based on its g -value, the low-field signal can be assigned to a positive polaron in P3HT (P^+). The high-field signal originates from a negative polaron in PCBM (P^-).

Simulations (dashed lines) were performed using the easyspin²¹ toolbox for Matlab (The MathWorks, Natick, MA) with the principal values of the g -matrices (2.0028 2.0019 2.0009) taken from Ref. 22 for P^+ in P3HT and (2.0003 2.0001 1.9982) taken from Ref. 23 for P^- in PCBM. While the simulation result agrees well with the measured spectra for short delays, we observe substantial differences for long delays. This discrepancy between simulation and measurement for P^+ in the trEPR signal was observed previously⁹ and can be explained with a not yet completely Boltzmann populated spin system for $7 \mu\text{s}$ delay after flash (DAF) at 80 K. For a complete relaxation of the polarization, the system needs $\sim 30 \mu\text{s}$ at this temperature.

For the CT state simulations, we assumed isotropic g -values (again based on Refs. 22 and 23) and weak isotropic coupling between the polarons. Note that while the interaction between the polaron spins is presumably dominated by (anisotropic) dipolar coupling, simulations based on isotropic coupling can reproduce the experimental CT state spectrum surprisingly well.⁹ We speculate that the averaging over many CT states with different relative orientation between the P^+ and P^- g -matrices results in a trEPR spectrum that looks like a spectrum from polaron pairs with isotropic spin coupling.

Fig. 2(b) (top) shows the color-coded transient EDMR spectrum of the solar cell close to flat-band conditions. Clear differences are observed as compared to the transient EPR spectrum, which are, among other points, related to the detection of the change of sample conductivity instead of

absorbed and emitted microwave radiation. This spectrum shows current quenching (Q: $\frac{\Delta I}{I} < 0$) as well as enhancing (En: $\frac{\Delta I}{I} > 0$) signal components. Since I is negative at a constant bias of ~ 0.77 V at 80 K, a negative current response corresponds to an enhancing signal and vice versa as shown in Fig. 3. Both data sets (trEPR and trEDMR) were background-corrected by the off-resonant microwave absorption and the photocurrent response after the laser flash, respectively.

The trEDMR spectrum for short DAF fits surprisingly well with the simulation assuming literature g -values for P3HT and PCBM. For this simulation, no coupling between both polarons was included because the coupling strength cannot be reliably extracted from the experimental spectrum. The inversion of the trEDMR signal measured between 0.4 and $7 \mu\text{s}$ is accompanied by a variation of the spectral shape detected for short and long delays ($0.4 \mu\text{s}$ as compared to $7 \mu\text{s}$). This change can be observed in the inset of Fig. 3, following the red and green vertical lines set to the maxima of the late spectrum. The EDMR spectrum at $7 \mu\text{s}$ DAF was simulated using again the complete anisotropic g -matrix for P^+ from literature, but for P^- only the g_z -component was used as the relevant g -value.

For the analysis of the time behavior of the trEDMR signals, three slices along the time axis at different resonant

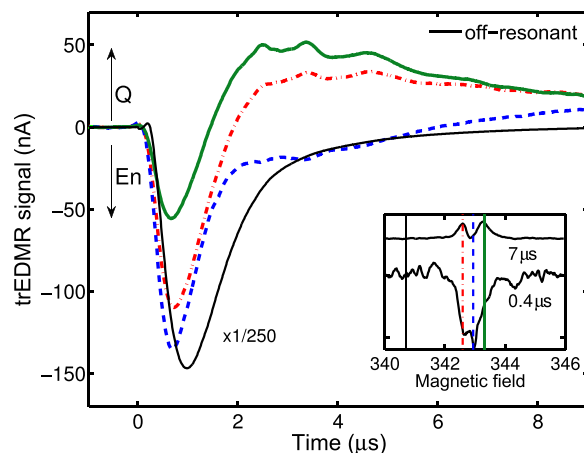


FIG. 3. Off-resonant current transient (solid black line) and background-corrected resonant transients recorded at different magnetic field positions (red dashed-dotted line, blue dashed line, and green solid line). The off-resonant transient is divided by a factor of 250 for better comparability.

magnetic field positions are given in Fig. 3. In addition, an off-resonant current transient (black solid line) is shown to visualize the background current response after the laser excitation. These background transients are subtracted from the trEDMR signals shown in Figs. 2 and 3. The resonant transients exhibit a transition from a current enhancing process (for short delays) towards a current quenching process (for long delays). Note that the off-resonant transient has a negative sign. The transition of the outer two transients occurs at a similar delay time as the transition from the CT state towards the purely absorptive signal seen in the trEPR measurement.

Our results demonstrate that trEPR and trEDMR measurements can be performed on fully processed solar cells under identical conditions. This paves the way for more detailed studies of the influence of paramagnetic centers on the photocurrent in thin-film solar cells.

The trEPR spectrum obtained from P3HT:PCBM bulk heterojunction solar cells at 80 K (Fig. 2(a)) shows the transition from the initial EAEA pattern (resulting from spin-correlated polaron pairs) towards a purely absorptive spectrum as expected for either separated non-interacting polarons or thermalized pairs with weak coupling. Distinguishing between the latter two species is not possible based on the information from trEPR alone. It is thus conceivable that the absorptive spectrum at $7\ \mu\text{s}$ originates from long-lived weakly coupled pairs that do not split up into separated charges and, in consequence, have no influence on the photocurrent. However, whether or not paramagnetic centers influence the photocurrent can directly be inferred from the trEDMR measurement (Fig. 2(b)). Here, we observe a resonant decrease of the photocurrent at $7\ \mu\text{s}$ DAF. This clearly shows that spin-dependent processes do affect the photocurrent. Yet, the trEDMR spectrum does not allow us to identify the underlying microscopic process. In particular, we are not able to discriminate between spin-dependent recombination of positive and negative polarons¹⁴ and spin-dependent hopping transport¹⁵ involving polymer segments that are temporarily occupied with two like-charge polarons. Both mechanisms could be active here and can possibly yield a quenching signal for the given bias voltage. In fact, which process dominates under distinct experimental conditions often remains a topic of controversy.^{24,25}

As the background-subtracted current transients shown in Fig. 3 reveal the transition from a current-enhancing to a current-quenching signal for some magnetic field positions, we presume that different spin-dependent mechanisms dominate the trEDMR spectrum on different time scales after the laser flash. An overshoot caused by the capacitance and the resistance of the sample may generally lead to a sign change of the trEDMR signal as well. However, the fact that the time behavior of the resonant current transients at different magnetic field positions varies substantially excludes this effect as a possible cause of the sign change. Note that the off-resonant current transient is negative throughout the whole time window shown in Fig. 3 (except for a small positive signal for short delays). A second indication for two processes, a current enhancing and a current quenching one, is that the spectral shape changes throughout the transition (cf. inset of Fig. 3).

The trEPR spectrum consists of an early spin-polarized CT state and late Boltzmann populated separated polaron states. The decay of the spin-polarized CT state is presumably dominated by the spin-lattice relaxation time of the spin states. The trEDMR and the trEPR spectra show similar decay and rise times for the early and late signals. This indicates that the trEDMR spectrum also arises from spin-polarized (early) and Boltzmann populated (late) states.

In the light of the present discussion on the identification of spin-dependent processes,^{24,25} we would like to emphasize that we clearly see a trEDMR signal centered at the g -value attributed to P^- in PCBM, confirming that the signal involves negative polarons in the fullerene phase. This g -value clearly differs from $g = 2.003$ which was suggested to be related to defect-induced paramagnetic centers in PCBM giving rise to room temperature EDMR signals in degraded PCBM films.²⁶

The resonant signals in the trEPR and trEDMR spectra at $t = 7\ \mu\text{s}$ can be attributed to P^+ in P3HT and P^- in PCBM.^{22,23} However, there are small but significant deviations between the trEPR and trEDMR measurements. All measurements can be simulated using g -matrices for both blend materials determined by light-induced EPR. Interestingly, we obtain excellent agreement between the measured trEDMR spectrum for long delays and the simulation assuming an isotropic line centered at g_z of photogenerated P^- in PCBM (as determined from light-induced EPR measurements). This may indicate that the EDMR intensity is mainly governed by polaron pairs comprising PCBM molecules (accommodating the P^-) with a preferential orientation with respect to the direction of the external magnetic field. A more detailed analysis of this phenomenon is currently being carried out.

Note that the trEDMR measurement does not allow us to resolve whether or not the polarons giving the trEPR spectrum at $7\ \mu\text{s}$ are already separated. However, the trEDMR measurements clearly show that the microwave manipulation of the spin states of positive and negative polarons influences the photocurrent for a delay of $7\ \mu\text{s}$ at low temperatures. The challenge of future experiments will be to face short spin relaxation times and to investigate trEDMR at room temperature.

In conclusion, this study demonstrates that trEDMR experiments at 80 K can provide information on paramagnetic species in fully processed organic solar cell devices that usefully complement the conclusions drawn from trEPR experiments. Our results show that the resonant signals observed in the trEDMR spectrum of P3HT:PCBM solar cells are consistent with the EPR line parameters of photogenerated P^+ in P3HT and P^- in PCBM,^{22,23} indicating that both centers are involved in spin-dependent processes that influence the device current.

We thank Dieter Neher and his group at the Universität Potsdam for helping us with the sample preparation and for the possibility to fabricate the EDMR solar cells in Potsdam. We acknowledge financial support from the DFG (SPP 1601) and the Helmholtz Association (Energie-Allianz Hybrid-Photovoltaik).

- ¹W. Brütting and C. Adachi, *Physics of Organic Semiconductors*, 2nd ed. (Wiley-VCH, Weinheim, 2012).
- ²N. S. Sariciftci, L. Smilowitz, A. J. Heeger, and F. Wudl, "Photoinduced electron-transfer from a conducting polymer to buckminsterfullerene," *Science* **258**, 1474–1476 (1992).
- ³S. Schaefer, S. Saremi, K. Fostiropoulos, J. Behrends, K. Lips, and W. Harneit, "Electrical detection of coherent spin pair oscillations in ZnPc devices," *Phys. Status Solidi B* **245**, 2120–2123 (2008).
- ⁴W. J. Baker, T. L. Keevers, J. M. Lupton, D. R. McCamey, and C. Boehme, "Slow hopping and spin dephasing of coulombically bound polaron pairs in an organic semiconductor at room temperature," *Phys. Rev. Lett.* **108**, 267601 (2012).
- ⁵A. Rao, P. C. Y. Chow, S. Gelinas, C. W. Schlenker, C. Z. Li, H. L. Yip, A. K. Y. Jen, D. S. Ginger, and R. H. Friend, "The role of spin in the kinetic control of recombination in organic photovoltaics," *Nature* **500**, 435–440 (2013).
- ⁶L. Pasimeni, L. Franco, M. Ruzzi, A. Mucci, L. Schenetti, C. Luo, D. M. Guldi, K. Kordatos, and M. Prato, "Evidence of high charge mobility in photoirradiated polythiophene-fullerene composites," *J. Mater. Chem.* **11**, 981–983 (2001).
- ⁷L. S. Swanson, J. Shinar, and K. Yoshino, "Optically detected magnetic-resonance study of polaron and triplet-exciton dynamics in poly(3-hexylthiophene) and poly(3-dodecylthiophene) films and solutions," *Phys. Rev. Lett.* **65**, 1140–1143 (1990).
- ⁸J. Niklas, K. L. Mardis, B. P. Banks, G. M. Grooms, A. Sperlich, V. Dyakonov, S. Beaupre, M. Leclerc, T. Xu, L. P. Yu, and O. G. Poluektov, "Highly efficient charge separation and polaron delocalization in polymer-fullerene bulk-heterojunctions: A comparative multi-frequency EPR and DFT study," *Phys. Chem. Chem. Phys.* **15**, 9562–9574 (2013).
- ⁹J. Behrends, A. Sperlich, A. Schnegg, T. Biskup, C. Teutloff, K. Lips, V. Dyakonov, and R. Bittl, "Direct detection of photoinduced charge transfer complexes in polymer fullerene blends," *Phys. Rev. B* **85**, 125206 (2012).
- ¹⁰F. Kraffert, R. Steyrlleuthner, S. Albrecht, D. Neher, M. C. Scharber, R. Bittl, and J. Behrends, "Charge separation in PCPDTBT:PCBM blends from an EPR perspective," *J. Phys. Chem. C* **118**, 28482–28493 (2014).
- ¹¹J. van Tol, L. C. Brunel, and R. J. Wylde, "A quasioptical transient electron spin resonance spectrometer operating at 120 and 240 GHz," *Rev. Sci. Instrum.* **76**, 074101 (2005).
- ¹²D. R. McCamey, H. Huebl, M. S. Brandt, W. D. Hutchison, J. C. McCallum, R. G. Clark, and A. R. Hamilton, "Electrically detected magnetic resonance in ion-implanted Si:P nanostructures," *Appl. Phys. Lett.* **89**, 182115 (2006).
- ¹³M. Stutzmann, M. S. Brandt, and M. W. Bayerl, "Spin-dependent processes in amorphous and microcrystalline silicon: A survey," *J. Non-Cryst. Solids* **266-269**, 1–22 (2000).
- ¹⁴D. R. McCamey, K. J. van Schooten, W. J. Baker, S. Y. Lee, S. Y. Paik, J. M. Lupton, and C. Boehme, "Hyperfine-field-mediated spin beating in electrostatically bound charge carrier pairs," *Phys. Rev. Lett.* **104**, 017601 (2010).
- ¹⁵J. Behrends, A. Schnegg, K. Lips, E. A. Thomsen, A. K. Pandey, I. D. W. Samuel, and D. J. Keeble, "Bipolaron formation in organic solar cells observed by pulsed electrically detected magnetic resonance," *Phys. Rev. Lett.* **105**, 176601 (2010).
- ¹⁶W. Ma, C. Yang, X. Gong, K. Lee, and A. J. Heeger, "Thermally stable, efficient polymer solar cells with nanoscale control of the interpenetrating network morphology," *Adv. Funct. Mater.* **15**, 1617–1622 (2005).
- ¹⁷S. T. Turner, P. Pingel, R. Steyrlleuthner, E. J. W. Crossland, S. Ludwigs, and D. Neher, "Quantitative analysis of bulk heterojunction films using linear absorption spectroscopy and solar cell performance," *Adv. Funct. Mater.* **21**, 4640–4652 (2011).
- ¹⁸Y. Kim, S. A. Choulis, J. Nelson, D. D. C. Bradley, S. Cook, and J. R. Durrant, "Device annealing effect in organic solar cells with blends of regioregular poly(3-hexylthiophene) and soluble fullerene," *Appl. Phys. Lett.* **86**, 063502 (2005).
- ¹⁹J. Schafferhans, A. Baumann, C. Deibel, and V. Dyakonov, "Trap distribution and the impact of oxygen-induced traps on the charge transport in poly(3-hexylthiophene)," *Appl. Phys. Lett.* **93**, 093303 (2008).
- ²⁰A. Sperlich, H. Kraus, C. Deibel, H. Blok, J. Schmidt, and V. Dyakonov, "Reversible and irreversible interactions of poly(3-hexylthiophene) with oxygen studied by spin-sensitive methods," *J. Phys. Chem. B* **115**, 13513–13518 (2011).
- ²¹S. Stoll and A. Schweiger, "EasySpin, a comprehensive software package for spectral simulation and analysis in EPR," *J. Magn. Reson.* **178**, 42–55 (2006).
- ²²A. Aguirre, P. Gast, S. Orlinskii, I. Akimoto, E. J. J. Groenen, H. E. Mkami, E. Goovaerts, and S. V. Doorslaer, "Multifrequency EPR analysis of the positive polaron in I-2-doped poly(3-hexylthiophene) and in poly[2-methoxy-5-(3,7-dimethyloctyloxy)]-1,4-phenylenevinylene," *Phys. Chem. Chem. Phys.* **10**, 7129–7138 (2008).
- ²³J. DeCeuster, E. Goovaerts, A. Bouwen, J. C. Hummelen, and V. Dyakonov, "High-frequency (95 GHz) electron paramagnetic resonance study of the photoinduced charge transfer in conjugated polymer-fullerene composites," *Phys. Rev. B* **64**, 195206 (2001).
- ²⁴C. Boehme and J. M. Lupton, "Challenges for organic spintronics," *Nat. Nanotechnol.* **8**, 612–615 (2013).
- ²⁵J. Behrends, I. D. W. Samuel, A. Schnegg, and D. J. Keeble, "Persistent spin coherence and bipolarons," *Nat. Nanotechnol.* **8**, 884–885 (2013).
- ²⁶H. Morishita, W. J. Baker, D. P. Waters, R. Baarda, J. M. Lupton, and C. Boehme, "Mechanisms of spin-dependent dark conductivity in films of a soluble fullerene derivative under bipolar injection," *Phys. Rev. B* **89**, 125311 (2014).